Fluorescence Studies of the Secondary Structure and Orientation of a Model Ion Channel Peptide in Phospholipid Vesicles†

Laura Ann Chung,‡ James D. Lear,* and William F. DeGrado*
Du Pont Central Research & Development Department and The Du Pont Merck Pharmaceutical Company, P.O. Box 80328, Wilmington, Delaware 19880-0328

Received December 16, 1991; Revised Manuscript Received April 10, 1992

ABSTRACT: A 21-residue peptide of the sequence $(LSSLLSL)_3$ forms ion channels when incorporated into planar lipid bilayer membranes of diphytanoylphosphatidylcholine (diPhy-PC). The frequency of channel openings increases with the applied voltage gradient. We investigated the molecular and structural mechanisms underlying this voltage dependence. A series of seven peptides, each containing a tryptophan substituted for a single residue in the middle heptad, was synthesized, purified, and incorporated into small, unilamellar, diPhy-PC vesicles. We measured circular dichroism, maximum fluorescence emission wavelengths, and fluorescence quenching by both aqueous and lipid hydrocarbon-associated quenchers. Circular dichroism spectra and the observed sequence periodicity of all fluorescence and fluorescence quenching data are consistent with an α-helical peptide secondary structure. Energy transfer quenching measurements using N-terminally labeled $(LSSLLSL)_3$ co-incorporated at lipid/peptide ratios > 100 into vesicles with one of the Trp-substituted peptides showed that the vesicle-associated peptide, in the absence of a voltage gradient across the bilayer, exists as an equilibrium mixture of monomers and dimers. Static fluorescence quenching measurements using different lipid-bound quenchers indicate that the helical axis of a representative lipid-associated peptide is, on average, oriented parallel to the surface of the membrane and located a few angstroms below the polar head group/hydrocarbon boundary. This surface orientation for the peptide is confirmed by the complementary sequence periodicity observed for Trp fluorescence emission wavelength shifts and collisional quenching by aqueous CsCl. The resulting model is consistent with a molecular mechanism for the observed voltage dependence of ion channel formation whereby a fraction of the helical peptide is induced by the transmembrane voltage gradient, to switch from a surface to a transmembrane orientation.

Electrical transmission in the nervous system involves proteins which allow Na^+, K^+, Ca^{2+}, and Cl^- ions to pass quickly and selectively across cell membrane bilayers. In most cases, these ion channel proteins are large polypeptides containing hundreds to thousands of amino acids [reviewed by Numa (1989)]. However, some small peptides are also capable of exhibiting ion channel activity. Examples include naturally occurring peptides such as alamethicin [reviewed by Hall et al. (1987)] and cecropins (Christensen et al., 1988), as well as totally synthetic peptides chosen to mimic transmembrane segments of natural channel proteins (Oiki et al., 1988; Grove et al., 1991). Although these peptides are small compared to the proteins from which they are derived, they still have a very large number of different possible structural arrangements because they contain many different amino acids in sequences with little apparent symmetry. Peptides designed from a "minimalist" approach (DeGrado et al., 1988), containing only leucine and serine in amphiphilic helical sequences 21 residues long, have also been shown to form well-defined ion channel conductance states (Lear et al., 1987). In particular, the sequence $(LSSLLSL)_3$ (Figure 1) was shown to form cation-selective channels with an apparent diameter of about 8 Å. The frequency with which these channels were observed (in planar bilayer experiments), but not their average open lifetime, depended on the applied transmembrane voltage. This voltage-dependent frequency of channel openings was particularly interesting because some natural channels and peptides also show voltage-dependent opening kinetics.

Figure 2 schematically depicts possible structural intermediates of a previously proposed (DeGrado & Lear, 1990) kinetic scheme to account for the voltage dependence of the $(LSSLLSL)_3$ peptide channel formation. In this model, essentially that proposed in early investigations of alamethicin (Baumann & Mueller, 1974), the voltage dependence of channel openings is related to a voltage-dependent partitioning between two different orientations of an amphiphilic, α-helical peptide in a fluid-phase lipid membrane. In the absence of a transmembrane voltage, the horizontal orientation depicted in Figure 2A is expected to be considerably more stable than the perpendicular orientation because the polar serine residues, designed to lie on the same side of the α-helix, can remain exposed to the aqueous exterior of the membrane while the apolar leucines on the other side can be buried in the bilayer hydrocarbon interior. However, because the α-helix has an effective charge of about $\pm^1/_2$ of an electronic charge unit at its N (+) and C (−) termini, respectively (Wada, 1977), introduction of a transmembrane electrical potential can reduce the energy difference between the parallel and perpendicular orientations. The electrostatic portion of the energy difference is just that of transferring one of the "end charges" to the different potential across the membrane. This general concept of dipole reorientation (Eisenberg et al., 1973; Kempf et al., 1982; Boheim et al., 1983; Hall et al., 1984) and electric field-dependent partitioning (Schwartz et al., 1986) has previously been postulated to explain the voltage dependence of bilayer conductance induced by peptides, including that of the channel-forming alamethicin. However, despite a number of interesting structural studies [e.g., Fox and Richards (1982),

† This work was supported in part by a grant from the United States Office of Naval Research.
* Corresponding authors.
‡ Current address: NIH/NIAID, Twinbrook II Facility; 12441 Parklawn Drive, Rockville, MD 20852.

0006-2960/92/0431-6608$03.00/0

```
      LSSLLSLLSSLLSLLSSLLSL-CONH2
W8L   LSSLLSLWSSLLSLLSSLLSL-CONH2
W9L   LSSLLSLLWSLLSLLSSLLSL-CONH2
W10L  LSSLLSLLSWLLSLLSSLLSL-CONH2
W11L  LSSLLSLLSSWLSLLSSLLSL-CONH2
W12L  LSSLLSLLSSLWSLLSSLLSL-CONH2
W13L  LSSLLSLLSSLLWLLSSLLSL-CONH2
W14L  LSSLLSLLSSLLSWLSSLLSL-CONH2
```

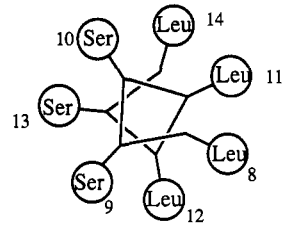

FIGURE 1: Peptide sequences for fluorescence and fluorescence quenching studies and an axial helical projection of the middle heptad sequence in the $(LSSLLSL)_3$ peptide showing the positions of Trp substitution.

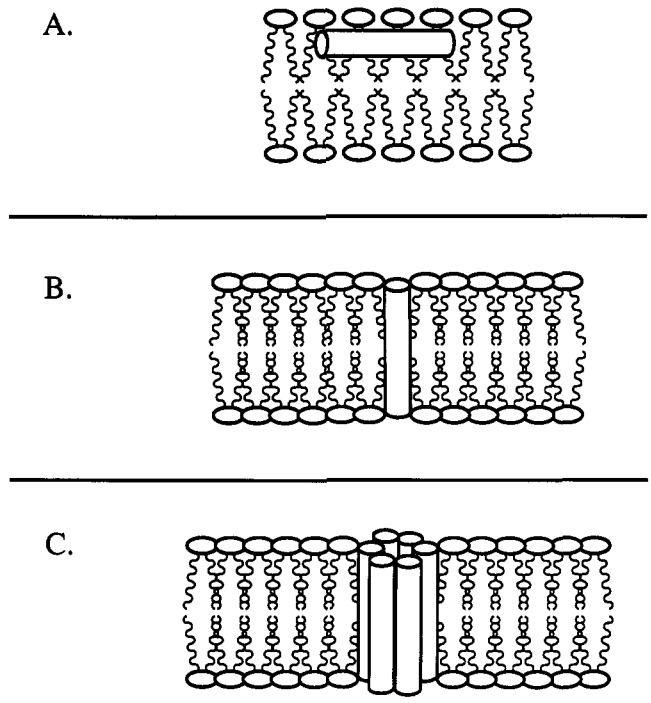

FIGURE 2: Proposed model for the voltage-dependent frequency of channel openings. (A) The major closed state for the peptide incorporated into lipid membranes in the absence of a voltage difference across the bilayer. The peptide is oriented parallel to the plane of the bilayer and located in or close to the lipid head group region of the membrane. (B) Change of peptide orientation from horizontal to transmembrane. A reorientation of the peptide occurs upon application of a voltage gradient to the membrane. The peptide "flips" from a surface to a transmembrane orientation due to alignment of the helical dipole moment with the electric field. (C) Formation of conducting ion channels by the transmembrane-oriented peptide. The transmembrane-oriented peptide aggregates, sequestering the polar seryl hydroxyls from the lipid acyl chains and creating polar pathways large enough to pass ions.

Huang et al. (1988), Wu et al. (1990), and Archer et al. (1991)], the secondary structure and orientation of alamethicin in bilayer membranes is still not known in enough detail to distinguish among many different proposed mechanisms of voltage gating [see discussion by Cascio and Wallace (1988)]. The inherent simplicity of the $(LSSLLSL)_3$ peptide sequence and channel behavior appeared to offer some promise for understanding the structural basis for its voltage-dependent channel formation, so we undertook this study.

To determine the secondary structure and orientation of $(LSSLLSL)_3$ in its predominantly closed state (the initial state depicted in Figure 2A), we used the approach of O'Neil et al. (1986), who investigated a series of calmodulin-binding peptides in which a Trp residue was placed sequentially at each position of the peptide. The environment-sensitive fluorescence properties of the peptides were found to vary with a 3.6-residue period, indicating that the peptides formed helices when bound to calmodulin. Similarly, Altenbach et al. (1990) used electron paramagnetic resonance spectroscopy to measure the oxygen accessibility of nitroxide spin labels attached to cysteine residues (incorporated by site-directed mutagenesis) at successive positions in bacteriorhodopsin to probe its structure in membranes. In the present work, we used a tryptophan residue successively substituted by peptide synthesis into each position of the central heptad of the $(LSSLLSL)_3$ sequence, giving a series of seven variant peptides, each containing only one fluorophore (Figure 1). Fluorescence studies were done using aqueous suspensions of fluid-phase phospholipid vesicles with high lipid/peptide mole ratios and no electrical potential gradient, conditions chosen to represent "closed states" of the ion channels previously observed in planar bilayer membranes.

Experimental Procedures

Materials Supply and Handling. All lipids were purchased from Avanti Polar Lipids, Birmingham, AL. Amino acids for peptide synthesis were purchased from Bachem, Torrance, CA, and Advanced Chemtech, Louisville, KY. Peptides and lipids were stored frozen and desiccated as lyophilized powders (greater than 1 month) or in methanol solutions in a 4 °C freezer (less than 1 month).

Peptide Synthesis and Purification. Peptides synthesized for this study are illustrated in Figure 1. The nomenclature employs the standard single-letter code for amino acids (W = Trp, L = Leu, S = Ser) and a notation adopted for site-directed mutagenesis studies of proteins (for example, W13S denotes a derivative of $(LSSLLSL)_3$ in which Trp replaces Ser at the 13th position in the amino acid sequence). Two of the tryptophan-containing channel peptides, W13S and W11L, were synthesized using FMOC chemistry on a 4-methylbenzhydrylamine resin and a combination of pentafluorophenyl and hydroxybenzotriazole esters and symmetric anhydrides of the respective protected amino acids [reviewed in Barany et al. (1987)]. The first five couplings were single reactions whereas the remaining amino acids required double couplings. The side chain protecting groups were removed with trifluoroacetic acid, and then the peptide was removed from the resin with anhydrous HF containing 10% anisole at 0 °C.

While the crude peptide had few side products as determined by reverse-phase analytical HPLC, the final yield of purified peptide was approximately 5%. Therefore, the remaining peptides were synthesized using conventional BOC chemistry with symmetric anhydrides. Peptides were purified with a semipreparative Vydac C4 column (The Separations Group, Hesperia, CA) using a gradient of increasing buffer B (acetonitrile/2-propanol/TFA (66.6%, 33.3%, 0.1%) with buffer A of 0.1% TFA in water. Peptides were repurified using a

semipreparative PRP-1 column (Pierce, Rockford, IL) eluted with a gradient of increasing acetonitrile in water containing 0.1% TFA. Purity of the peptides was checked by fast atom bombardment mass spectrometry (FAB MS) and analytical HPLC. Final yields of purified peptides synthesized using BOC chemistry were approximately 10–15% on the basis of the loadings of the first amino acid to the resin.

Dansyl and Pyrenyl Labeling of (LSSLLSL)$_3$ Peptide. The peptides were reacted with 1.1 equivalents of dansyl chloride or 1-pyrenyl isothiocyanate and 2.0 equivalents of triethylamine in DMSO/methanol (1:1) for between 24 and 72 h. The resulting products were purified by reverse-phase HPLC as described above.

Incorporation of Peptide into Lipid Vesicles. A modified ethanol injection procedure rather than sonication was used for all fluorescence samples to avoid possible heating and oxidation. A mixture of lipid and peptide dissolved in ethanol was injected into a 5 mM phosphate buffer solution (pH = 7.0 ± 0.3) with rapid vortexing as described previously (Batzri & Korn, 1973; Kremmer et al., 1977). The vesicle sizes for a few representative samples were characterized using quasielastic light scattering (QELS) and electron microscopy. The majority of vesicles had diameters ranging from 300 to 800 Å. Since our fluorescence measurements were not expected to be particularly sensitive to vesicle size in this range, we did not perform a size separation of the vesicles, but rather we used the samples as prepared.

Preparation of Collisional Quenching Samples. Samples were prepared by first making up peptide/lipid/ethanol injection solutions having mole ratios of approximately 1:100 peptide/lipid for each of the tryptophan-containing peptides using diphytanoylphosphatidylcholine as the lipid. Stock solutions for background samples lacked peptide. These solutions were injected into 1.5 mL of 5 mM sodium phosphate buffer (pH 7.0 ± 0.3) containing the appropriate concentration of CsCl. Additional NaCl was added to bring the total salt concentration to a constant value of 1 M for all samples. Samples were prepared in duplicate with final concentrations of ethanol = 1% (v/v), lipid = 176 μM, and peptide = 1.5 μM. Fluorescence emission spectra of samples with and without 1 M added NaCl showed no differences in maximum emission wavelengths or shapes, indicating no salt-induced change in the peptides' tryptophan environment. Stern–Volmer quenching plots (F_o/F versus CsCl concentration) were linear up to 0.8 M CsCl.

Preparation of Samples for Maximum Fluorescence Emission Wavelength Measurements. Stock injection solutions were prepared as described for the collisional quenching measurements except samples were made up in triplicate. Stock solutions of peptide and lipid in ethanol were injected into 1.5 mL of 5 mM sodium phosphate buffer (pH = 7.2 ± 0.1). Final concentrations of lipid, peptide, and ethanol were as for collisional quenching samples.

Energy Transfer Sample Preparation and Measurements. Separate vesicle preparations were made from different ethanolic stock solutions of peptide and lipid for individual fluorescence intensity measurement points. The ethanolic solution containing diphytanoylphosphatidylcholine, W12L peptide, and dansyl-(LSSLLSL)$_3$ (or pyrenyl-(LSSLLSL)$_3$) peptide. The mole fraction of W12L mixed with dansyl-(LSSLLSL)$_3$ was varied from 0 to 1, keeping the lipid to total peptide ratio constant in separate experiments at either 150, 300, or 1200. In separate control experiments, unsubstituted (LSSLLSL)$_3$ was used in place of the dansylated peptide. Samples were prepared in triplicate by injecting stock solutions into 1.5 mL of 5 mM sodium phosphate buffer, pH 7.1 ± 0.1. Final concentrations of ethanol = 1% (v/v), diphytanoylphosphatidylcholine = 0.2 mM, and total peptide = 1.3 μM. The tryptophan fluorescence intensity was measured as a function of the mole fraction of W12L peptide at room temperature using a SPEX 222 Fluorolog spectrofluorometer in the ratio mode with λ_{ex} = 285 nm, slit = 1.6 nm (band-pass), path = 1 cm and λ_{em} = 340 nm, slit = 5.4 nm, path = 4 mm, for the pyrenyl peptide; and with λ_{ex} = 285 nm and λ_{em} = 340 nm with both slits = 1.25 nm and both paths = 4 mm for the dansyl peptide. The background fluorescence was estimated using a second set of samples containing the lipid, dansyl, or pyrenyl peptide and underivatized (LSSLLSL)$_3$ (as a substitute for W12L). The background-corrected, averaged intensities were normalized to give a value of 1.0 when the mole fraction of W12L is 1.0.

Preparation of Samples for Depth Quenching Measurements. Stock solutions and samples were prepared as for the oligomeric energy transfer assay. Each stock solution comprised a tryptophan-containing peptide and diphytanoylphosphatidylcholine with varying proportions of one of the spin-labeled lipids. The molar ratio of spin-labeled lipid to diphytanoylphosphatidylcholine was varied from 0 to 1 to explore the functional dependence of quenching on quencher concentration. Peptide/lipid mole ratios and final concentrations of ethanol, lipid, and peptide were the same as for the collisional quenching assay except no salt was added to sample solutions. Absorbance of samples for both excitation and emission wavelengths was checked; inner filter effects were neglible.

Circular Dichroism. Samples were prepared and measured as described by DeGrado and Lear (1990).

Results

Peptides. The peptides shown in Figure 1 were synthesized by stepwise solid-phase peptide synthesis and purified to apparent homogeneity by a two-step procedure using reverse-phase HPLC. They had very low water solubilities and therefore could only be studied spectroscopically as dispersions in lipid. The modified peptides were incorporated into small, unilamellar vesicles of diphytanoylphosphatidylcholine at a peptide/lipid ratio of 1:100 or 1:150. Under these conditions, in the absence of a transmembrane potential, little or no channel activity was expected. The fluorescent properties of the peptides were then measured under different conditions, and the results, discussed in detail below, were correlated with residue position in the primary sequence.

Circular Dichroism Measurements. Because the peptides contain only 21 amino acid residues, the replacement of even one residue with a tryptophan could affect their secondary structure. We therefore measured circular dichroism spectra of the parent peptide (LSSLLSL)$_3$ and substitution peptides W11L and W13S. The spectra were essentially identical to those previously reported for (LSLLLSL)$_3$ (DeGrado & Lear, 1990) with residue molar ellipticities at 222 nm (θ_{222}) of, respectively, −22 650, −18 990, and −20 640 deg·cm^2/dmol. The slightly lower ellipticity of the Trp-containing peptides might be the result of positive contributions of the aromatic side chains to the CD spectrum (Woody, 1978). The similarity of the circular dichroism spectra indicates that replacement of a single residue in the original peptide sequence does not radically perturb the secondary structure of these peptides when they are incorporated into lipid vesicles. In addition, the ion channel voltage gating properties of the W11L peptide were found, in limited experiments, to be qualitatively similar to the original peptide's properties (data not shown).

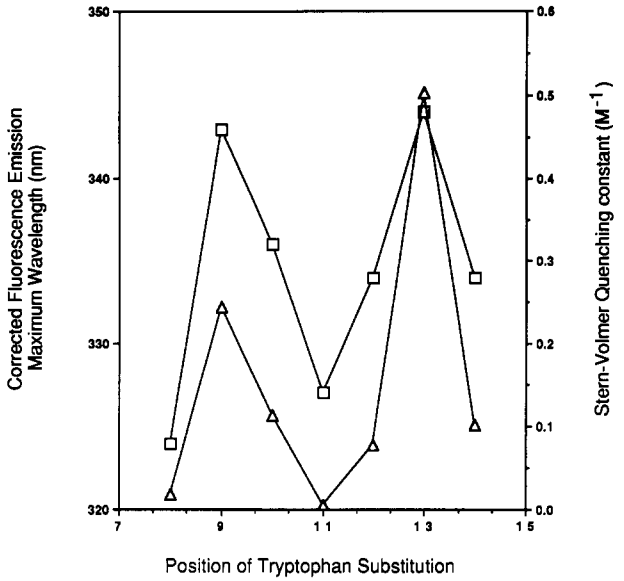

FIGURE 3: Fluorescence emission wavelength maxima and aqueous quenching by cesium ions versus the position of tryptophan substitution in the peptide primary sequence. Squares indicate the maximum emission wavelengths and triangles indicate the aqueous quenching (Stern–Volmer constants) of the peptides. An excitation wavelength of 285 nm was used for the spectroscopic measurements of all peptides, and the emission spectra were corrected for variations in photomultiplier response.

Tryptophan Emission Spectra. The first fluorescence parameter examined was the maximum emission wavelengths of each tryptophan-containing peptide incorporated into small phospholipid vesicles. The lower the value of the tryptophan emission maximum, the more hydrophobic is the environment of the tryptophan (Bursten et al., 1973; Lakowicz, 1983). For the series of peptides examined here, the measured maximum emission wavelengths (Figure 3) show the environment experienced by the Trp residues to vary in a periodic pattern, which follows that expected for a helical structure as demonstrated previously (O'Neil et al., 1987). The λ_{max} values for tryptophans in serine-replaced positions are red-shifted toward values expected for a more polar environment than those in the leucine positions. It should be noted that none of the tryptophan-containing peptides gave emission maxima as great as that (352 nm) for free tryptophan in aqueous solution (Lakowicz, 1983). This suggests that the peptide is embedded deeply enough in the bilayer so that the Trp residues on the serine side of the helix are within the headgroup region of the surface.

Aqueous Phase Quenching. To confirm that the serine positions were more exposed to the aqueous phase than the leucine positions, collisional fluorescence quenching by a water-soluble quencher was employed. Cesium ion (as CsCl) was used as a "heavy atom" aqueous quencher for tryptophan residues in proteins (Altekar, 1974). Although its fluorescence quenching is weak, Cs^+ is not expected to partition readily into the acyl chain region of the bilayer. The quenching results for each of the tryptophan-containing peptides are plotted along with the above-described λ_{max} values in Figure 3. The periodic pattern is paralleled for both measurements, and both aqueous quenching and λ_{max} are greatest at the serine 13 position. It can be seen in Figure 1 that this position would be furthest from the membrane interior if the peptide were to be oriented with its long helical axis parallel to the bilayer surface. Although all of the serine positions exhibit more aqueous quenching than seen for the leucine positions, the highest calculated Stern–Volmer quenching rate constant (0.5 M^{-1} for W13S) is considerably less than that reported for Cs^+ quenching of free L-tryptophan in solution [3 M^{-1} calculated for a 2.7-ns lifetime from Eftink and Ghiron (1981)]. The decrease in the diffusion coefficient of the fluorophore on the vesicle-bound peptide might account for at most half of this difference. The remaining difference could arise from the more restricted zone of approach angle for Cs^+ quenching the membrane-bound Trp, although some contribution from steric restrictions in the head group region cannot be ruled out.

Tryptophan Emission Quenching from Lipid Phase. The peptide's orientation and location with respect to the membrane bilayer was determined using a technique recently developed for localizing fluorophores covalently bound to lipids (Chattopadhyay & London, 1987). This technique, now referred to as the "parallax method", determines the distance of a fluorophore from the center of the bilayer by static fluorescence quenching of the fluorophore by quenching groups covalently bound at defined positions on lipid acyl chains. Here, we measure specifically each peptide's tryptophan fluorescence in lipid vesicles as a function of the mole fraction of a series of lipids, each bearing a nitroxide quencher at a defined position on one of its acyl chains (see Figure 4). The equation describing this dependence is derived from a two-dimensional form of the Perrin equation [see Birks (1970)] for static quenching and predicts a simple exponential dependence of quenching on the mole fraction of quencher:

$$F/F_0 = \exp[-\pi\ (C/70)(R_0^2 - X^2 - Z^2)] \qquad (1)$$

where C is the mole fraction of quencher molecules ($C/70$ gives the number of quencher molecules/Å^2 assuming that the cross-sectional area of a lipid molecule is 70 Å^2); R_0 is the "hard sphere" critical radius for quenching; X is the quencher–fluorophore closest possible lateral distance; and Z is the quencher–fluorophore closest possible vertical distance.

As expected from eq 1, the quenching of the peptides by the nitroxide-containing lipids is well described by a single exponential. Figure 5 illustrates a plot of ln (F/F_0) versus the mole fraction (of 5-doxyl lipid) for W8L and W13S. These plots are linear over the 0 to 1 mole fraction range, although for some peptide–quencher pairs, some deviations from linearity were noted beyond a mole fraction of 0.5. Linear regression for each fluorophore–quencher pair between 0 and 0.5 mole fraction gives the value of $(\pi/70)(R_0^2 - X^2 - Z^2)$ as the regression coefficient, allowing the value Z to be calculated if R_0 and X are known. Alternatively, the value of Z can be calculated directly without R_0 and X being known using the parallax method.

The parallax method uses the assumption that R_0 and X remain constant for a given quencher–fluorophore pair differing only in the closest approach distance, Z. The value of $R_0^2 - X^2 - Z_a^2$ determined for one nitroxide (a), located at a known distance Q_a (Figure 4B) from the bilayer center, is subtracted from the value $R_0^2 - X^2 - Z_b^2$ determined for another nitroxide (b) located at a different position, Q_b, giving $Z_b^2 - Z_a^2$. Once this difference is known, the distance of the fluorophore from the bilayer center (P), can be calculated[1]

[1] The simplest form of the derived equation for calculating distances (which we have used in this work) assumes that the critical quenching radius for the fluorophore–quencher pair is less than the transleaflet separation (equivalent to assuming all quenching occurs between pairs localized to the same leaflet of the bilayer). In our work, this assumption was justified since the residue closest to the bilayer center (the leucine 11 position) was calculated to be 14 Å away from the closest spin-label position in the transleaflet, outside the 12-Å critical quenching radius estimated for the Trp-doxyl pair (London & Feigenson, 1981).

from

$$P = [Z_b^2 - Z_a^2 + Q_a^2 - Q_b^2]/[2(Q_a - Q_b)] \quad (2)$$

The values of Q for the various nitroxides were taken from Chattopadhyay and London (1986) for the 5-, 10-, and 12-doxyl lipids. That for the 7-doxyl lipid was estimated by interpolation.

Measurements done in this work employed four rather than two different spin-label positions on the lipid acyl chain in order to cover (and possibly overlap for improved accuracy) a wide range of possible fluorophore locations in the bilayer. Peptides with Trp substituted at serine positions 9, 10, and 13 gave too little quenching with the 12-doxyl lipid for reliable results, so these combinations were not used. In addition, we found that the use of 5/7-doxyl quenching pairs in the parallax calculation gave results excessively deviant from the mean of the results from other pairs. Consequently, our analysis uses only data for doxyl pairs separated by more than two carbon atoms.

Figure 6 shows distances of the Trp residues from the center of the bilayer (P) for each peptide, calculated using the parallax method. The data are well described by a sine function with a period of 3.8, close to the period of the α-helix (3.6). The amplitude of the function is approximately 5 Å, which is in good agreement with the approximate radius (including side chains) of the α-helix. The data clearly indicate that the peptide is bound with its long helical axis parallel to the plane of the bilayer and located a few angstroms below the head group/hydrocarbon boundary. A transmembrane orientation would give a substantially different distribution of distances from the bilayer center.

Determination of Peptide Aggregation State. The aggregation state of the peptide under our experimental conditions was estimated using a fluorescence quenching method developed previously to establish the oligomeric state of bacteriorhodopsin in membranes (London & Khorana, 1982). This method requires two derivatives of a given peptide or protein, one bearing a fluorescent label and the other bearing a quencher of this fluorophore. If the two peptides form a hetero-oligomer, the emission of the fluorophore will be quenched by the presence of the quencher in the complex. If the peptides are predominantly present in a unique aggregation state at a given peptide concentration (as opposed to a mixture of monomers and higher order oligomers), the aggregation number can be determined by an experiment in which the two peptides are mixed such that the fraction of the fluorescent peptide is varied from 0 to 1.0, while simultaneously the fraction of the quencher peptide is varied from 1.0 to 0 such that the total concentration of the quencher plus the fluorescent peptide is constant. The fluorescence intensity, F, is measured as a function of the concentrations of the fluorescent derivative, [W] and the quenching derivative, [Q]. F is related to the aggregation number (n) according to

$$F/F_o = ([W]/([W] + [Q]))^n \quad (3)$$

where F_o is the fluorescence intensity in the absence of quencher. The equation assumes that the distribution of W and Q in the aggregates follows a binomial distribution and that the presence of even a single quencher is sufficient to cause complete quenching of all the fluorophores within a given aggregate. Thus, plotting log (F/F_o) versus log ([W]/([W] + [Q])) should give a linear relationship of slope n. If the peptides are present as a mixture of monomers and oligomers of varying n, the above equation can still be used if the presence of the fluorophore and quencher does not greatly affect the monomer/n-mer equilibrium. However, the experimentally determined value of n could be nonintegral.

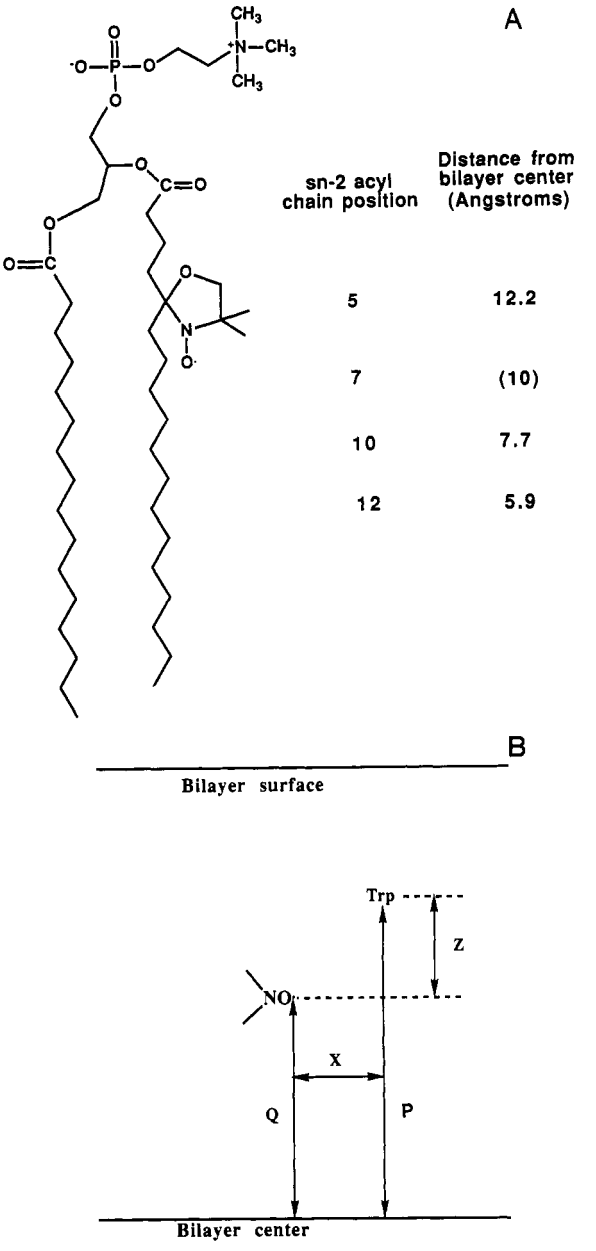

FIGURE 4: (A) Chemical structure of spin-labeled lipids [1-palmitoyl-2-(n-doxylstearoyl)phosphatidylcholines (n = position of doxyl in the stearoyl chain)] used in parallax depth quenching method. The nitroxide group is shown at acyl chain position 5. Estimated distances of the nitroxide from the bilayer center, Q (Chattopadhyay & London, 1986), are also indicated. (B) Summary of the geometric parameters used to calculate P, the distance from the bilayer center.

To determine n for the $(LSSLLSL)_3$ peptides, we used two different quenchers: either an N-terminal dansyl group or a pyrene group, both of which were attached to $(LSSLLSL)_3$. This was done to determine if different quenching groups attached to the peptide had different effects on oligomerization. As a fluorophore, we chose W12L. Figure 7A shows log (F/F_o) versus log ([W]/([W] + [Q])) for the peptide W12L paired with the "blank" quencher $(LSSLLSL)_3$ and with the quencher dansyl-$(LSSLLSL)_3$ at peptide/lipid mole ratios of 1:1200 and 1:300. As expected, the plots are linear and of unitary slope for the nonquenching blank, reflecting a simple dependence of measured intensity on the concentration of the tryptophan-containing peptide. In contrast, when the dansyl-$(LSSLLSL)_3$ peptide is substituted for $(LSSLLSL)_3$, the value of n determined by linear regression for the dansyl-

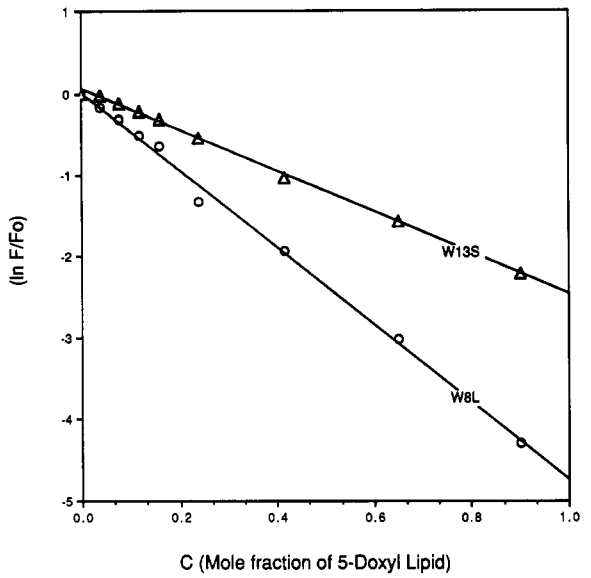

FIGURE 5: Representative fluorescence depth quenching curves for the W8L (open circles) and W13S (open triangles) as a function of the fraction of 5-doxyl quencher lipid in diphytanoyl-PC vesicles. Equation 1, describing static quenching of a membrane-bound fluorophore, predicts the linearity of ln (F/F_o) versus quencher lipid mole fraction observed for both peptides and indicates that the Trp of W8L can come closer to the quencher than the Trp of W13S.

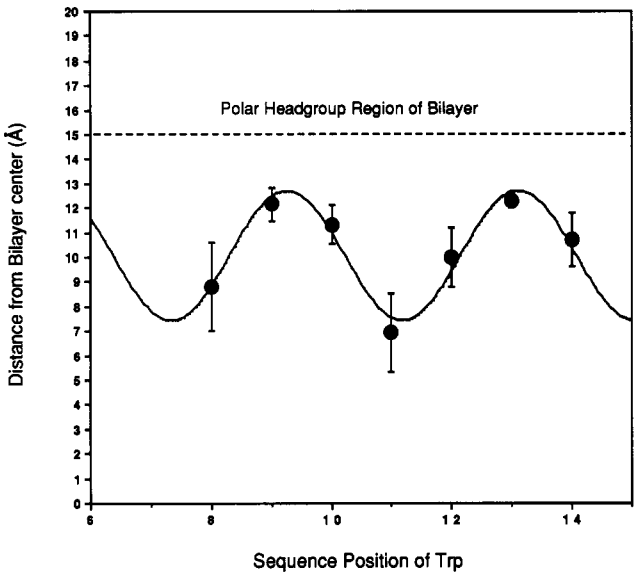

FIGURE 6: Calculated average tryptophan distance from the bilayer center versus the position of substitution in the peptide primary sequence. For each peptide, values of P, the distance of the fluorophore from the bilayer center, were calculated for selected quencher pairs (see text). These values were averaged for each peptide and the resulting mean distance ± its standard deviation are plotted here versus the replaced residue position. The solid line is a cosine function fit to the data: $y = D + A\cos[(2\pi/B)(x - C)]$. Parameters determined from nonlinear least-squares analysis: A = −2.6 ± 0.4; B = 3.8 ± 0.1; C = −12 ± 0.1; D = 10 ± 0.2.

$(LSSLLSL)_3$/W12L pair is 1.3 at a peptide/lipid ratio of 1:1200, suggesting that the peptide existed in a monomer/n-mer equilibrium with a high population of the monomeric species. If this is the case, the degree of association should be increased at higher peptide to lipid ratios. Indeed, at a peptide/lipid ratio of 1:300 the value of n is shifted to 1.7.

The degree of association showed a small dependence on the N-terminal quenching group. Data similar to the above were obtained for the pyrenyl peptide, but a value of n = 1.4 was calculated for quenching by the pyrenyl peptide derivative

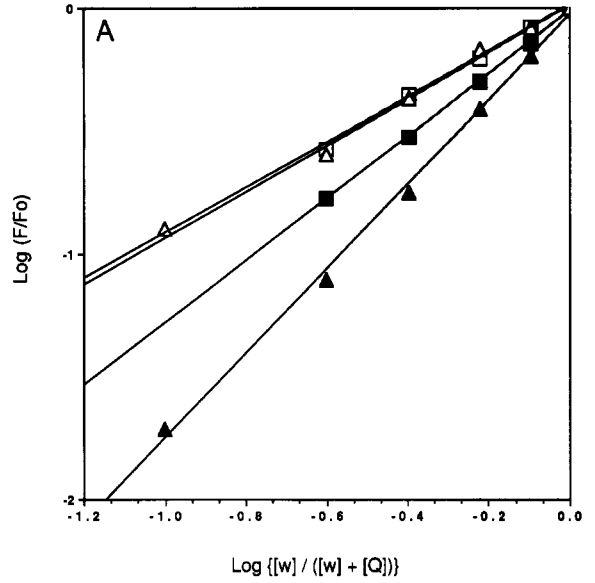

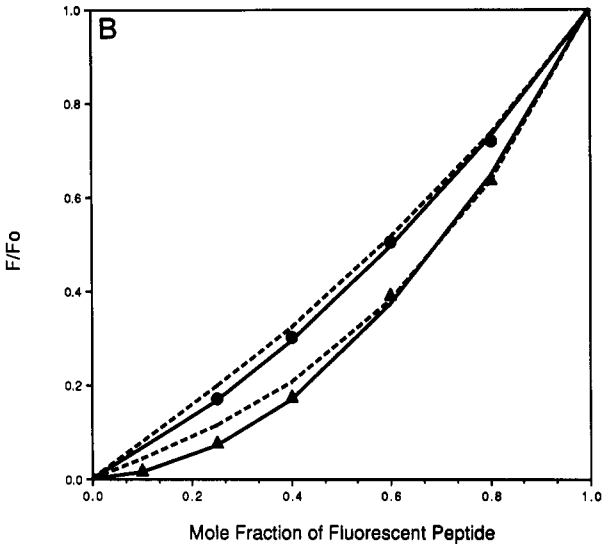

FIGURE 7: (A) Log of the fluorescence intensity (corrected for background and normalized to unit intensity at unit mole fraction W12L peptide) versus the log of the mole fraction of Trp-substituted peptide mixed with unlabeled (open symbols) or dansyl-labeled (solid symbols) $(LSSLLSL)_3$ peptide in vesicles prepared with peptide/lipid mole ratios of 1:1200 or 1:300. Calculated values of n determined by linear regression for unlabeled peptides: 0.94 (open squares, 1:1200) and 0.92 (open triangles, 1:300). For the dansylated peptides, values of n: 1.3 (solid squares, 1:1200) and 1.7 (solid triangles, 1:300). (B) Comparison of calculated and observed F/F_o values for the two different L/P ratios (triangles, L/P = 300; circles, L/P = 1200) where the calculated values are for monomer–dimer (solid line) and monomer–trimer (dashed line) equilibria. The K_{diss} values (concentration unit is peptide molecules/Å^2) used for the calculation were K_{diss} = 5.7×10^{-4} Å^{-2} for n = 2 and K_{diss} = 1.2×10^{-4} Å^{-4} for n = 3. These were chosen by first regression fitting the two individual L/P experiments to either n = 2 or n = 3 equilibrium relationships, then averaging the two "best-fit" values in order to minimize the deviations of observed and calculated F/F_o values at both L/P ratios.

at a peptide/lipid mole ratio of 1:150.

The observed, nonintegral values of n indicate that the peptide exists in an equilibrium between monomers, dimers, and possibly higher order aggregates. To determine the aggregation number of the self-associated species it is useful to consider the extension of eq 3 to multiple equilibria:

$$F/F_o = \Sigma x_n([W]/([W] + [Q]))^n \qquad (3a)$$

where x_n represents the fraction of the molecules in a given

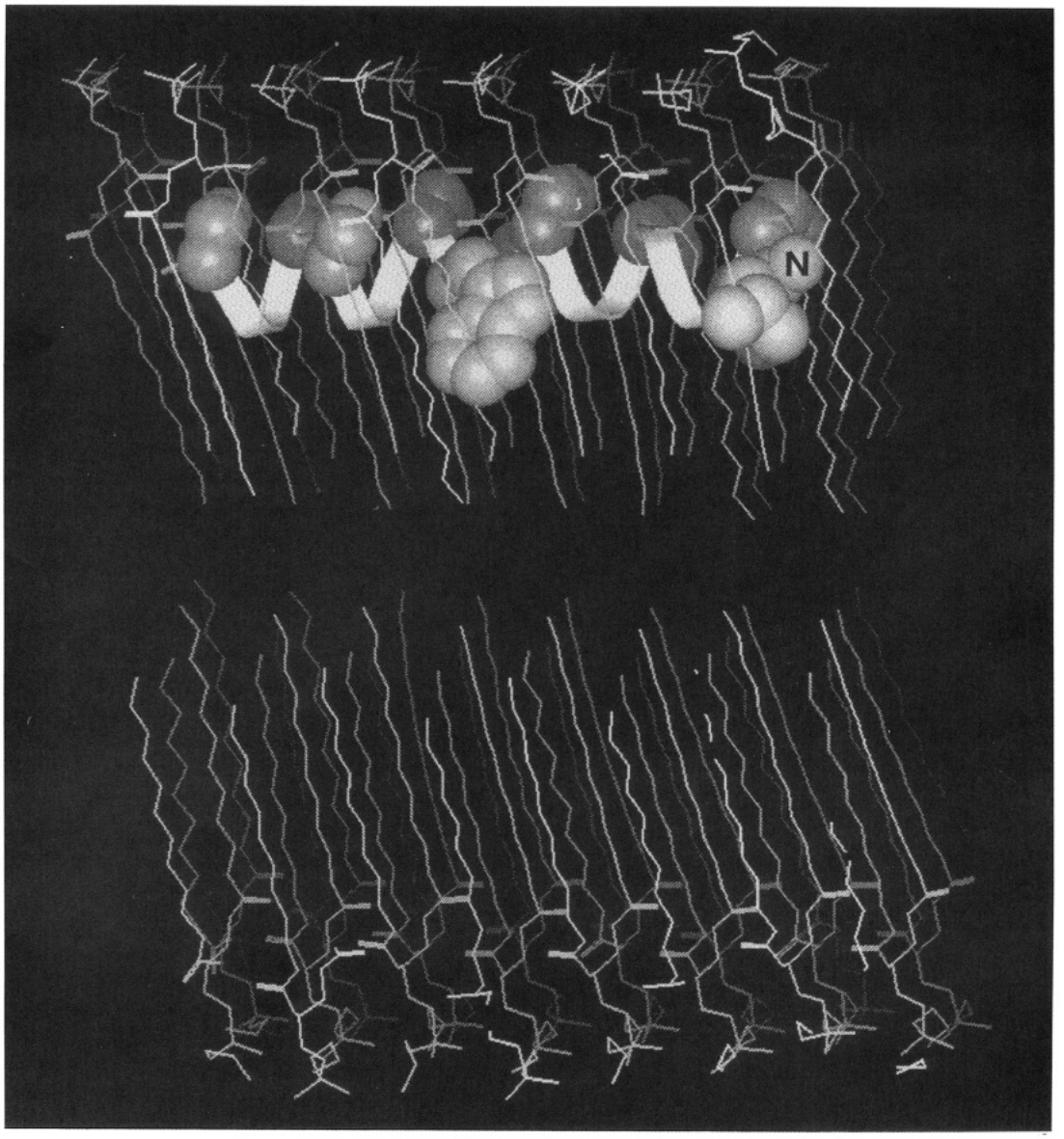

FIGURE 8: Helical ribbon model of the W12L peptide superimposed on a model of dilauroyl- (C_{12}) phosphatidylethanolamine on the basis of the lipid's crystal structure (Hitchcock et al., 1974) using the program Insight on a Silicon Graphics workstation. The upper and lower halves of the bilayer crystal structure were separated from their actual spacing by approximately 3 Å to better represent the hydrocarbon region thickness of a fluid-phase diPhy bilayer. In an actual fluid-phase bilayer, the lipids would be less well ordered, particularly around the peptide. Serine residues, the tryptophan group at position 12, and the N-terminal leucine group (oriented for favorable interface exposure) are shown with van der Walls surfaces.

aggregation state, the subscript refers to the number of molecules within that aggregation state, and the sum is taken over all aggregation states that are significantly populated. As a first approximation, we assume that only two aggregation states are present (the monomer and some other aggregated species), which leads to

$$F/F_o = x_m([W]/([W] + [Q])) + (1 - x_m)([W]/([W] + [Q]))^n \quad (3b)$$

where x_m is the fraction of the peptide that is in the monomeric state.

Equation 3b should, in principle, allow n and x_m to be calculated directly from the data by nonlinear regression. However, we found that, within experimental error, the data at each peptide/lipid ratio could be described as either a monomer/dimer or a monomer/trimer equilibrium using different values of x_m. To uniquely determine x_m, data from both peptide/lipid ratios were used to calculate n-mer dissociation constants for different values of n in the monomer/n-mer dissociation equilibrium relationship:

$$K_{diss} = [p_m]^n/[p_n] = ((x_m)^n[p_t]^n)/((1 - x_m)[p_t]/n) = (nx_m^n[p_t]^{n-1})/(1 - x_m) \quad (4)$$

where $[p_m]$, $[p_n]$, and $[p_t]$ are the surface concentrations of the monomer, the n-mer aggregate, and the total surface peptide concentrations (expressed in peptides per Å^2), respectively. This equation relates x_n, which is a concentration-dependent parameter, to K_{diss}, which is independent of concentration. Thus, a single value of K_{diss} should be obtainable that will accurately predict the data described in Figure 7A at both peptide/lipid ratios. To accomplished this, we used the ROOT function of MLAB (Knott, 1979) to formally solve eq 4 for x_m as a function of n, K_{diss}, and $[p_t]$, substituted this function into eq 3b, and used the MLAB FIT function to determine least-squares regression fit K_{diss} values for $n = 2$, 3, and 4 separately for data at each peptide/lipid

ratio. The two resulting values of K_{diss} for each n were then averaged, and the theoretical values for F/F_0 versus [W]/([W] + [Q]) were recalculated for the different values of n. This process was repeated with values of K_{diss} half way between the average and the extremes to determine if values different than the average value might give improved fits. For our purposes (to determine the best value of n), we found the average K_{diss} to serve adequately. Figure 7B illustrates the differences in calculated versus observed values of F/F_0 versus [W]/([W] + [Q]) for the two different peptide-to-lipid ratios using the average K_{diss} values calculated for $n = 2$ and 3. The monomer/dimer equilibrium (solid lines) gives an excellent fit to the data, while the monomer/trimer equilibrium (dashed lines) gives a poor fit.

Discussion

The combined results of several different spectroscopic experiments give a molecular view of the $(LSSLLSL)_3$ peptide in a fluid phase, voltage gradient-free lipid membrane that is consistent with previously observed voltage- and concentration-dependent ion channel forming properties. The α-helical structure of the peptide is established by CD spectroscopy and by the observed 3.5-residue periodicity of the tryptophan emission maxima and quenching by both aqueous Cs^+ and membrane-embedded nitroxide groups. The maximum fluorescence emission wavelengths and aqueous quenching by Cs^+ show that the peptide's polar serine positions are exposed to the aqueous compartment whereas the apolar leucines are sequestered in a hydrophobic compartment, consistent with the designed amphiphilic helical nature of the peptide sequence. Measurements of tryptophan fluorescence quenching by lipid-localized quenchers further confirm the disposition of the serine and leucine positions at the bilayer head group/hydrocarbon interface. This technique predicts that the long helical axis of the peptide is parallel to, and located a few angstroms below, the head group/hydrocarbon boundary of the bilayer. Figure 8 illustrates this geometric arrangement with approximate reference to actual tryptophan residue, N-terminal leucine, and lipid bilayer dimensions.

There are a few technical points related to the interpretation of the lipid-phase quenching data in terms of quantitative geometric dimensions which need to be addressed. For quenching of membrane-bound fluorophores attached to specific lipid acyl chain positions, the inherent uncertainty in the method due to the fluid nature of the bilayer is about ±4 Å (Wiener & White, 1991). Also, peptide side chains undergo rapid position fluctuations in the bilayer, as has been reported for 21-residue Aib-containing model peptides (Vogel et al., 1988). For quenching induced by the paramagnetic nitroxides, the extent of quenching is expected to depend on distance (although the relationship is not established; Green et al., 1990). Consequently, calculated "hard sphere" distances should not be interpreted as representing rigid geometric positions. Finally, the distances were calculated assuming that the lipid acyl chains were fully extended, although both thermal motion and the presence of the peptide would be expected to affect the order and orientation of lipid hydrocarbon chains. The resolution of the data we obtain is, therefore, about the best that can be expected.

A second point to note about the data is that all these calculations assume a single orientation for the peptide in the bilayer. Peptide partitioned between two different orientation states with different distances of the Trp from the bilayer center would show up in the parallax method as a multiple exponential quenching versus mole fraction curve, something we do not observe. However, in practice, it would be difficult to detect contributions from a minor population of less than 10% of a different peptide orientation. Therefore, a small percentage of peptide in a transbilayer configuration could remain undetected by these methods.

The finding of a horizontal orientation of the peptide applies specifically to the $(LSSLLSL)_3$, which was designed to have a rather strict lateral segregation of polar and apolar residues in an α-helical conformation. Thus, it is not surprising to find that the majority of the peptide appears to be oriented parallel to the polar/apolar interface because this orientation allows maximal hydration of the Ser hydroxyl groups and simultaneous dehydration of the Leu isobutyl side chains. Other peptides, with different sequences, might well bind to bilayers in other orientations and at different depths depending on the specific peptide sequence. For example, qualitative tryptophan depth quenching studies have been reported (Voges et al., 1987) on peptides representing the apolar 20-residue peptide $(Ala\text{-}Aib\text{-}Ala\text{-}Aib\text{-}Ala)_4$. In this case, the predominant orientation of the peptide in lipid vesicles appears to be transmembrane. Also, it should be emphasized that the studies of $(LSSLLSL)_3$ described in this paper were conducted at relatively low peptide/lipid ratios, which should stabilize the monomeric and dimeric surface-absorbed forms of the peptide. At significantly higher peptide/lipid ratios, we would expect the more highly associated forms of the peptide such as the transmembrane helical bundle shown in Figure 2 to be more stable.

An unexpected finding was that dansyl- and pyrenyl-$(LSSLLSL)_3$ are partially dimeric under our experimental conditions. In this context, it is interesting to note that, in its crystal structure, melittin forms a tight dimer of α-helices with a clean segregation of hydrophobic and hydrophilic residues. This highly amphiphilic dimer was postulated to bind to peptide bilayers with the α-helical axes parallel to the bilayer surface (Terwilliger et al., 1982). $(LSSLLSL)_3$ can form a similar, amphiphilic dimer by associating to form an antiparallel coiled-coil of α-helices or a parallel coiled-coil (leucine zipper) motif (O'Shea et al., 1991) (Figure 9). Thus, it is likely that both the dimeric and monomeric forms of $(LSSLLSL)_3$ would bind to the membrane in the same horizontal orientation, explaining the clean depth-quenching results that we obtain for this peptide.

Finally, it is important to emphasize that, although the voltage dependence of the opening and closing kinetics of $(LSSLLSL)_3$ ion channels shows some similarities to the channel behavior of large cellular membrane proteins, it is unlikely that their mechanisms of opening and closing are the same. The major reorientation of helices proposed for the relatively small and mobile $(LSSLLSL)_3$ peptide is considerably more difficult to envision for larger ion channel proteins such as the acetylcholine receptor. On the other hand, the similarities we do see with peptide and protein ion channels could reflect underlying structural similarities. Of particular interest are the transmembrane helical packing requirements; residues which change the relative stabilities of different helix packing interfaces in the ion channel forming peptide may do the same in a large channel protein with observable consequences on gating and/or conduction behavior. Experimental studies of peptides with sequences closely related to those discussed here are in progress to help define the effects of differences in peptide channel structure on ion channel characteristics.

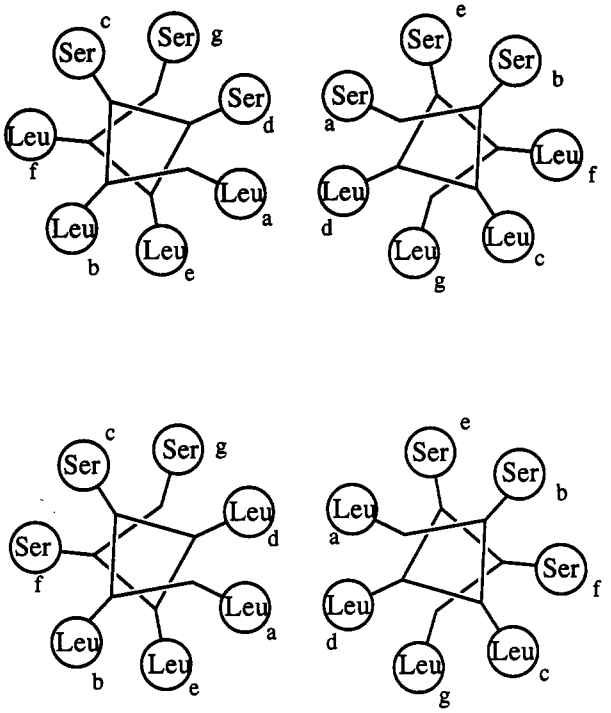

FIGURE 9: Two potential α-helical coiled-coil conformations for the peptide $(LSSLLSL)_3$. The illustrated heptad repeat units of the dimerization motifs begin at different residues of each individual peptide, so the dimerization motifs would be limited to less than the full length of the peptide. In both of the dimers shown here, the spatial segregation of hydrophobic Leu residues and hydrophilic Ser residues is strikingly well-suited for an interfacial location.

ACKNOWLEDGMENTS

We gratefully acknowledge Daniel Camac for conductance measurements and assistance in purification of the peptides, Karyn O'Neil for amino acid analyses, Robert Flippen for QELS measurements, Robert van Kavelaar for electron microscopy, Joseph Lazar for FAB MS analyses, James Krwyko and Carl Hodge for computer graphics, Erwin London for the use of equipment at SUNY—Stonybrook for spin-label quantitation, and Amitabha Chattopadhyay, Erwin London, and Maria Rafalski for helpful discussions and comments.

Registry No. $(LSSLLSL)_3$, 115921-69-2; diPhy-PC, 64626-70-6.

REFERENCES

Altekar, W. (1974) *FEBS Lett. 49*, 208–211.
Altenbach, C., Marti, T., Khorana, H. G., & Hubbell, W. L. (1990) *Science 248*, 1088–1092.
Archer, S. J., Ellena, J. F., & Cafiso, D. S. (1991) *Biophys. J. 60*, 389–398.
Barany, G., Kneib-Cordonier, W., & Mulen, D. G. (1987) *Int. J. Pept. Protein Res. 30*, 705–739.
Bartlett, G. (1959) *J. Biol. Chem. 234*, 466–468.
Batzri, S., & Korn, E. (1973) *Biochim. Biophys. Acta 298*, 1015–1019.
Baumann, G., & Mueller, P. (1974) *J. Supramol. Struct. 2*, 538–557.
Birks, J. B. (1970) *Photophysics of Aromatic Molecules*, pp 341–347, Wiley-Interscience, London.
Boheim, G., Hanke, W., & Jung, G. (1983) *Biophys. Struct. Mech. 9*, 181–191.
Bursten, E. A., Vendenkina, N. S., & Ivkova, M. N. (1973) *Photochem. Photobiol. 18*, 263–279.
Cascio, M., & Wallace, B. A. (1988) *Proteins: Struct., Funct., Genet. 4*, 89–98.
Chattopadhyay, A., & London, E. (1987) *Biochemistry 26*, 39–45.
Christensen, B., Fink, J., Merrifield, R. B., & Mauzerall, D. (1988) *Proc. Natl. Acad. Sci. U.S.A. 85*, 5072–5076.
DeGrado, W. F., & Lear, J. D. (1990) *Biopolymers 29*, 205–213.
DeGrado, W. F., Wasserman, Z. R., & Lear, J. D. (1988) *Science 243*, 622–628.
Eftink, M. R., & Ghiron, C. A. (1981) *Anal. Biochem. 114*, 199–227.
Eisenberg, M., Hall, J. E., & Mead, C. A. (1973) *J. Membr. Biol. 14*, 143–176.
Fox, R. O., & Richards, F. M. (1982) *Nature (London) 300*, 325–330.
Green, S. A., Simpson, D. J., Zhou, G., Ho, P. S., & Blough, N. V. (1990) *J. Am. Chem. Soc. 112*, 7337–7346.
Grove, A., Tomich, J. M., & Montal, M. (1991) *Proc. Natl. Acad. Sci. U.S.A. 88*, 6418–6422.
Kempf, C., Klausner, R. D., Weinstein, J. N., Van Renswoude, J., Pincus, M., & Blumenthal, R. (1982) *J. Biol. Chem. 257*, 2469–2476.
Knott, G. D. (1979) *Comput. Programs Biomed. 10*, 271–280.
Hall, J. E., Vodyanoy, I., Balsubrumanian, T. M., & Marshall, G. B. (1984) *Biophys. J. 45*, 233–247.
Hitchcock, P. B., Mason, R., Thomas, R. M., & Shipley, G. G. (1974) *Proc. Natl. Acad. Sci. U.S.A. 71*, 3036–3040.
Kremmer, J. M. H., Esker, M. J. W., Pathmamanoharan, C., & Wiersema, P. H. (1977) *Biochemistry 17*, 3932–3935.
Lakowicz, J. R. (1983) *Principles of Fluorescence Spectroscopy*, Plenum, New York.
Lear, J. D., Wasserman, Z. R., & DeGrado, W. F. (1987) *Science 240*, 1177–1181.
London, E., & Feigenson, G. W. (1981) *Biochemistry 20*, 1932.
London, E., & Khorana, H. G. (1982) *J. Biol. Chem. 257*, 7003–7011.
Numa, S. (1989) *The Harvey Lectures, Series 83*, pp 121–165, Alan Liss, New York.
Oiki, S., Danho, W., Madison, V., & Montal, M. (1988) *Proc. Natl. Acad. Sci. U.S.A. 85*, 8703–8707.
Olah, G. A., & Huang, H. W. (1988) *J. Chem. Phys. 89*, 2531–2538.
O'Neil, K. T., Wolfe, H. R., Erickson-Viitanen, S., & DeGrado, W. F. (1987) *Science 236*, 1454–1456.
O'Shea, E. K., Klemm, J. D., Kim, P. S., & Alber, T. (1991) *Science 254*, 539–544.
Schwarz, G., Stankowski, S., & Rizzo, V. (1986) *Biochim. Biophys. Acta 219*, 253–262.
Terwilliger, T. C., Weissman, L., & Eisenberg, D. (1982) *Biophys. J. 37*, 353–361.
Vogel, H., Nilsson, L., Rigler, R., Voges, K., & Jung, G. (1988) *Proc. Natl. Acad. Sci. U.S.A. 85*, 5067–5071.
Voges, K., Jung, G., & Sawyer, W. H. (1987) *Biochim. Biophys. Acta 896*, 64–76.
Wada, A. (1977) *Adv. Biophys. 9*, 1–63.
Wang, S., Martin, E., Cimino, J., Omann, G., & Glaser, M. (1988) *Biochemistry 27*, 2033–2039.
Wiener, M. C., & White, S. H. (1991) *Biochemistry 30*, 6997–7008.
Woody, R. W. (1978) *Biopolymers 17*, 1451–1467.
Wu, Y., Huang, H. W., & Olah, G. A. (1990) *Biophys. J. 57*, 797–806.